BeBeC-2026-S11

BENCHMARK FOR ACOUSTIC SOURCE LOCALIZATION OF FLYOVER MICROPHONE ARRAY MEASUREMENTS

Timo Schumacher[1] and Henri Siller[1]
[1]German Aerospace Center (DLR), Institute of Propulsion Technology, Engine Acoustics Department
Bismarckstr. 101, 10625 Berlin, Germany

Abstract

The localization of acoustic sources of aircraft in flight is a core challenge for beamforming methods since they have first been used in the early 1990s independently by Bryce, Michel and Botcher. It has remained a field of active research, where different groups have applied similar methods to reconstruct the noise levels of aircraft components. However, the details of the methods themselves as well as the implementations may differ. Until now, no flyover microphone array dataset has been made broadly accessible to the research community. With this publication, we will make a data set available of a flyover recording of the DLR ATRA research aircraft, an Airbus 320-232. The recording was made in 2016 in the context of the Low Noise ATRA Project, which aimed to test noise reduction approaches. This particular recording was chosen because in this configuration, several aeroacoustic sources on the airframe and engine are present. The dataset contains the calibrated pressure signals from a large array of the DLR-Engine Acoustics Department with 238 microphones, arranged in logarithmic spirals. The arrangement is stretched in the direction of fligt, resulting in a diameter of 43 m along the longer, 36 m on the shorter side. The aircraft velocity above ground was 88 m/s and the altitude was 180 m above the array. The dataset is provided in the HDF5-file format that is organized according to the structure used for the exchange of microphone array data in the past. Here, it is extended to accommodate the trajectory of the aircraft as well. Due to the movement of the aircraft and source region, data for the trajectory in the form of waypoints and reference times is provided. In this talk and publication, we will present the methods used by our research team and the results we were able to accomplish with them. .

1 INTRODUCTION

As part of the Low Noise ATRA Campaign, several flyovers of the DLR ATRA research aircraft, an Airbus 320-232, were recorded [7]. The data is provided in HDF5 format. A pistonphone

was used to calibrate the micorophones. In addition to the already calibrated microphone data, the dataset also contains other necessary metadata (as datasets or attributes) required for analysis. The metadata includes, among other things, the microphone data, information on measured wind speed, temperature, and air pressure, as well as the assumed movement of the aircraft. This documentation serves to provide a more detailed explanation and clear presentation of the information already contained in the file. The "Analysis" chapter at the end of this documentation provides an overview of how the data is further processed within the DLR-Engine Acoustics Department.

2 DATA DESCRIPTION

File Structure

The HDF5 file has a hierarchical structure. The following diagram shows the arrangement of the most important information.

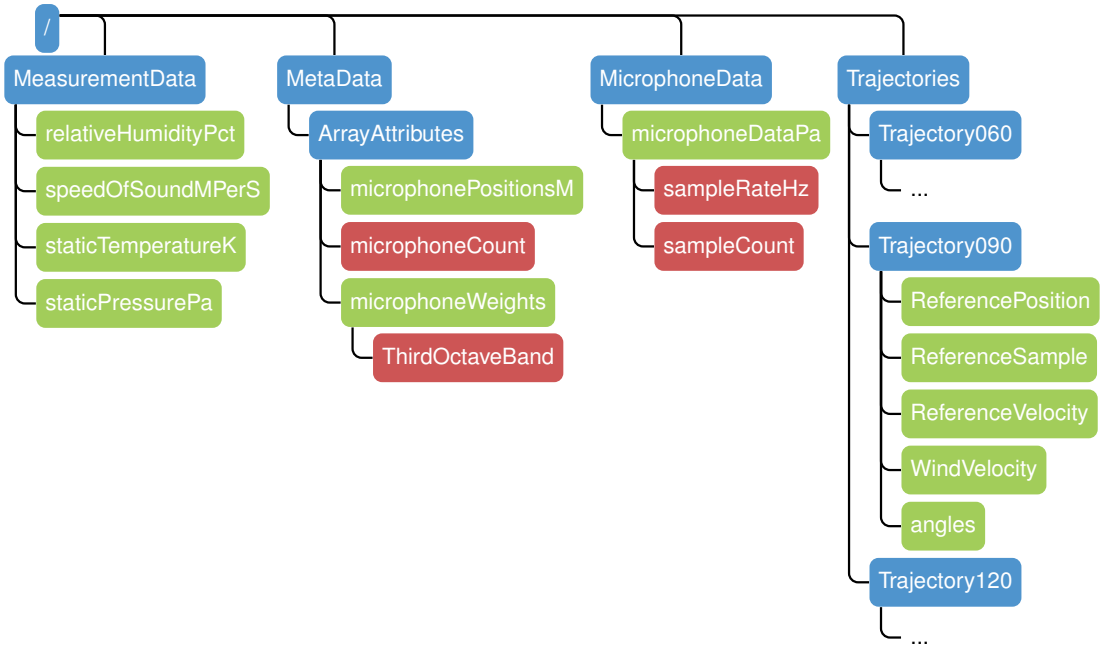

Figure 1: The internal structure of the provided hdf5-datafile. Groups are shown in blue, data sets in green, and attributes in red.

2.1 Coordinate System

All position and velocity data are with respect to the local coordinate system. The system is fixed in space and follows the right-hand rule. The origin is at the center of the array. The $\mathbf{e}_x$-axis is parallel to the runway in the eastward direction, $_z$ is vertical.

2.2 Microphone Locations

The dataset contains the signals of 238 calibrated microphones, arranged in logarithmic spirals (see fig. 2). The arrangement is stretched in the direction of flight to increase the resolution for shallow angles. This results in a diameter of 43 m along the longer, 36 m on the shorter side. The microphone positions where measured with high accuracy using a *total station* by Leica Geosystems. The microphones are applied close to the ground using small clips glued to the airports tarmac, so that hard-walled, non-reverberant reflection can be assumed.

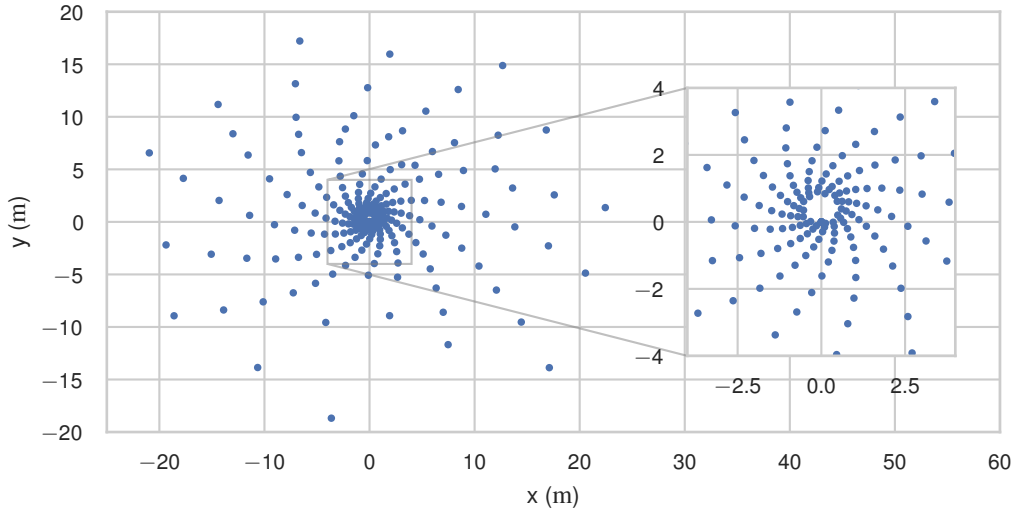

Figure 2: The microphones are arranged in logarithmic spirals. Some faulty channels are excluded from the datasets.

2.3 Trajectory

The *Trajectory* references a point at the center of the aircraft. It is linearized so that it can be represented by some reference position $\mathbf{x}_R$, velocity $\mathbf{v}_R$ and time $t_R = \frac{n_R}{f_s}$. The position is then given as

$$\mathbf{x}(t) = (t - t_R)\mathbf{v}_R + \mathbf{x}_R$$

which applies primarily in a region around t_R ($|t - t_R|$ is small). For short time intervals, this assumption is justified by the high inertia of the source.

Three linear trajectories are specified, each representing the best approximation of the trajectories for different sections of the flyover. Their identifiers refer to the emission angles 60°, 90°, 120° and correspond to the approach, overflight, and departure section of the same recording

However, the speed remained very constant in Record 139, so this distinction may be negligible, and the 90° trajectory can be used.

2.4 Aircraft Orientation

In addition to position data, the used flight log also contains information on the aircraft's orientation to transform points of the rigid body (the aircraft) to the local coordinate system.

The orientation is specified using extrinsic Euler angles in the form $(X-Y-Z)$. While they are based on the heading, elevation and bank angles, here they are specified with respect to the local coordinate system and their orientation also follows the right-hand rule (see fig. 3). This results in a large value of φ_3 which is close to 180°, as the flight direction and nose of the aircraft are close to antiparallel to the
mathbfe_x-axis. To clarify the distinction, the angles are referred to below as φ_x ,φ_y , and φ_z. All values are provided in degrees (°).

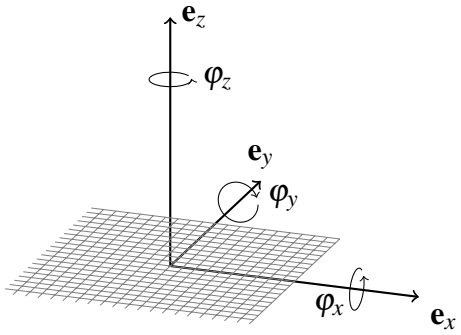

Figure 3: The provided orientation angles are required to transform points on the rigid body of the aircraft to the global coordinate system of the microphone array. They are all defined in the mathematical positive sense.

2.5 Wind Velocity

A wind velocity vector $\mathbf{u} = (u_x, u_y, 0)^T$ was calculated with respect to the local coordinate system from a recorded average wind speed and direction. Since it was taken from the flightlog for each of the three specified trajectories, there are also three wind velocity vectors available, which are stored together with the trajectories.

3 Analysis at DLR

3.1 Analysis Intervals

The source localization methods implemented in PSM2 assume direction-independent sources. To study the directional characteristics of the aircraft in flight, the recording is not evaluated as a whole but rather in various (short) emission time intervals, for which the sources are assumed to be constant and direction-independent.

These intervals are defined by the emission angle (see fig. 4), so that angle falls within some region around the nominal emission angle. In the presented case, this region $\Delta\theta = 10°$. I.e. the results labeled 90° are based on the sources within $\theta \in [85°, 95°]$. Table 2 presents the calculated emission times based on this scheme and the resulting time length of the evaluation.

Table 1: The aircrafts trajectory is provided as three linearized trajectories.

Trajectory		60°	90°	120°
Reference Sample		89926	152624	210406
→ Reference Time t_0 (s)		≈ 1.87	≈ 3.17	≈ 4.37
Reference Position $\mathbf{x}_R$ (m)	x_1	124.7	8.8	-97.1
	x_2	2.2	0.0	-1.1
	x_3	198.6	186.2	175.4
Reference Velocity $\mathbf{v}_R$ (m/s)	v_1	-88.0	-88.0	-88.0
	v_2	-0.3	-0.5	-0.5
	v_3	-9.4	-9.2	-8.7
Orientation Angle (°)	φ_1	-1.5	-0.6	0.2
	φ_2	7.4	6.9	6.6
	φ_3	182.2	182.6	182.4
Wind Velocity $\mathbf{u}$ (m/s)	u_1	1.8	1.7	1.7
	u_2	3.9	4.5	4.2

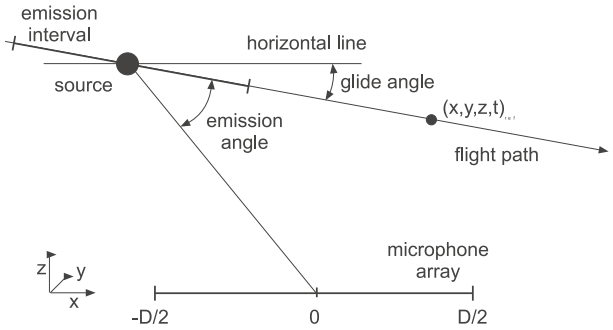

Figure 4: Definition of the emission angle

3.2 Dedopplerization and Conventional Time Domain Beamforming

As initial step, a dedopplerization through resampling is applied to the source grid's origin [4]. The measured amplitude is affected by the propagation through the atmosphere. This atmospheric attenuation can be compensated, using the model described in the standard ISO-9613-1 [1].

The conventional delay-and-sum beamforming method in the time domain was applied to the data. To increase the beamforming resolution and adapt the array properties to different frequency ranges, the contribution of each microphone was adapted using weighting factors, sometimes called shading [6]. Similar to using subarrays, they allow us to emphasize outer microphones at low frequencies and the center microphones at high frequencies. The weighting factors used are provided in the *microphoneWeights* dataset, one for each microphone and thid-octave band.

The source maps for the third-octave bands from 250 Hz to 5000 Hz for all three emission time intervals are provided in the appendix.

Table 2: The boundaries of the evaluated intervals.

	60°		90°		120°	
(θ_a, θ_b)	55°	65°	85°	95°	115°	125°
(t_a, t_b) (s)	2.181	2.424	3.394	3.576	4.551	4.793
Δt (s)	0.242		0.182		0.243	

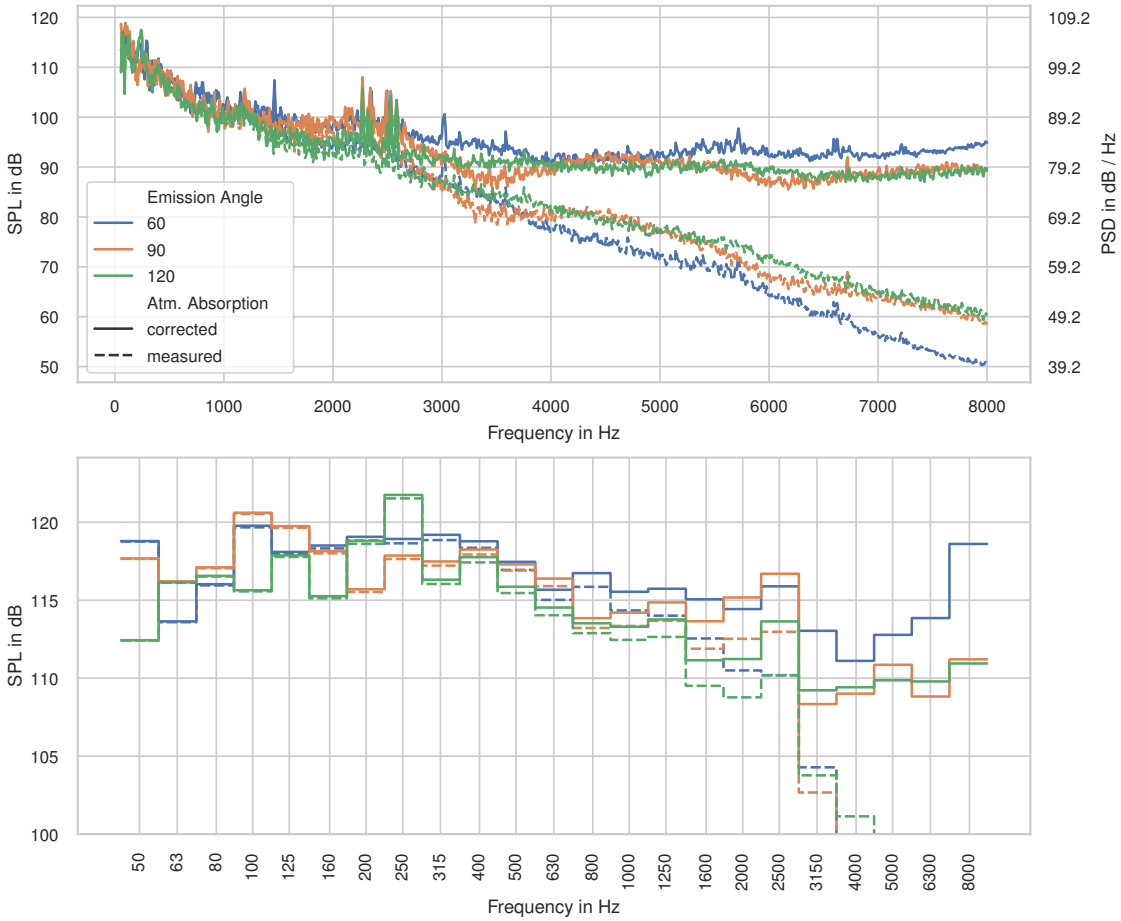

Figure 5: The dedopplerization results. The spectrum has a frequency resolution of $\Delta f = 8\,\mathrm{Hz}$.

4 SUMMARY

We have provided a microphone array recording of a measured flyover. The information in the dataset as well as this publication provide all required information to apply source localization methods and test their suitability with respect to aircraft flyovers.

The provided example results consist of a dedopplerized spectra as well as beamforming

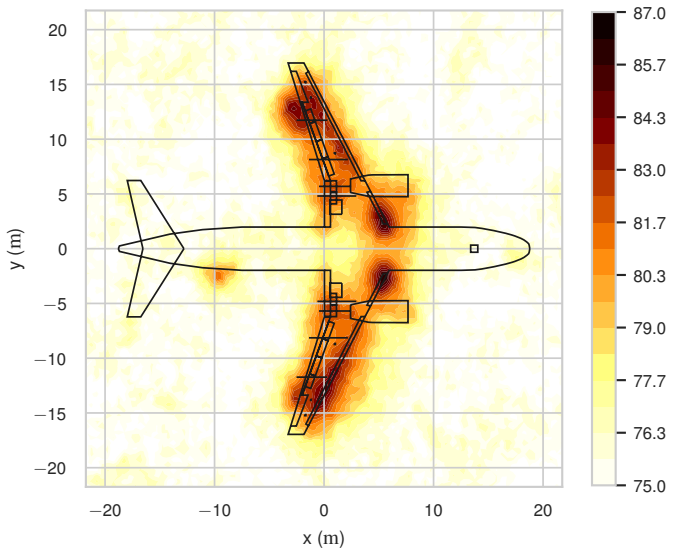

Figure 6: Beamforming results of the 90° *interval in the* 4000 Hz *third-octave band.*

results. The source maps allow for a separation of sources and follows the contour of the fuselage well, with noticeable sources at the intersections of wings and body (slathorns). The engines are the dominant sources at around 2.5 kHz.

In the past, similar benchmarks have shown, that even identical methods, implemented and used by individual research groups, resulted in different results [5]. We hope this benchmark initiates comparisons and discussions between research groups. Such discussions should include higher order methods, such as the hybrid deconvolution [3] and CLEANT [2].

The dataset is available on Zenodo.org

5 REFERENCES

REFERENCES

[1] "ISO 9613-1 – Acoustics – Attenuation of Sound During Propagation Outdoors.", 1993.

[2] R. Cousson, Q. Leclère, M.-A. Pallas, and M. Bérengier. "Identification of acoustic moving sources using an time-domain method." In *Proceedings on CD of the 7th Berlin Beamforming Conference, March 5-6, 2018*. GFaI, Gesellschaft zu Förderung angewandter Informatik e.V., Berlin, 2018. ISBN 978-3-942709-20-0. URL `http://www.bebec.eu/Downloads/BeBeC2018/Papers/BeBeC-2018-D17.pdf`.

[3] S. Guérin and C. Weckmüller. "Frequency-domain reconstruction of the point-spread function for moving sources." In *Proceedings on CD of the 2nd Berlin Beamforming Conference, 19-20 February, 2008*. GFaI, Gesellschaft zu Förderung angewandter Informatik e.V., Berlin, 2008. ISBN 978-3-00-023849-9. URL http://www.bebec.eu/Downloads/BeBeC2008/Papers/BeBeC-2008-14_Guerin_Weckmueller.pdf.

[4] G. P. Howell, M. A. Bradley, M. A. McCormick, and J. D. Brown. "De-Dopplerization and acoustic imaging of aircraft Flyover noise measurements." *J. Sound Vib.*, 105(1), 151–167, 1986. doi:10.1016/0022-460X(86)90227-0.

[5] E. Sarradj, G. Herold, P. Sijtsma, R. Merino Martinez, T. F. Geyer, C. J. Bahr, R. Porteous, D. Moreau, and C. J. Doolan. "A Microphone Array Method Benchmarking Exercise using Synthesized Input Data." In *23rd AIAA/CEAS Aeroacoustics Conference*. American Institute of Aeronautics and Astronautics. ISBN 978-1-62410-504-3. doi:10.2514/6.2017-3719. URL https://arc.aiaa.org/doi/10.2514/6.2017-3719.

[6] T. Schumacher. "Evaluation of microphone array methods for aircraft flyover measurements: Quantification of performance through virtual test environments." In *Fortschritte Der Akustik - DAGA 2022*, pages 784–787. Deutsche Gesellschaft für Akustik e.V. (DEGA). ISBN 978-3-939296-20-1. URL https://pub.dega-akustik.de/DAGA_2022.

[7] H. A. Siller, T. Schumacher, and W. Hage. "Low noise ATRA - phased array measurements of jet noise in flight." In *AIAA AVIATION 2021 FORUM*. American Institute of Aeronautics and Astronautics, 2021. doi:10.2514/6.2021-2160.

6 APPENDIX

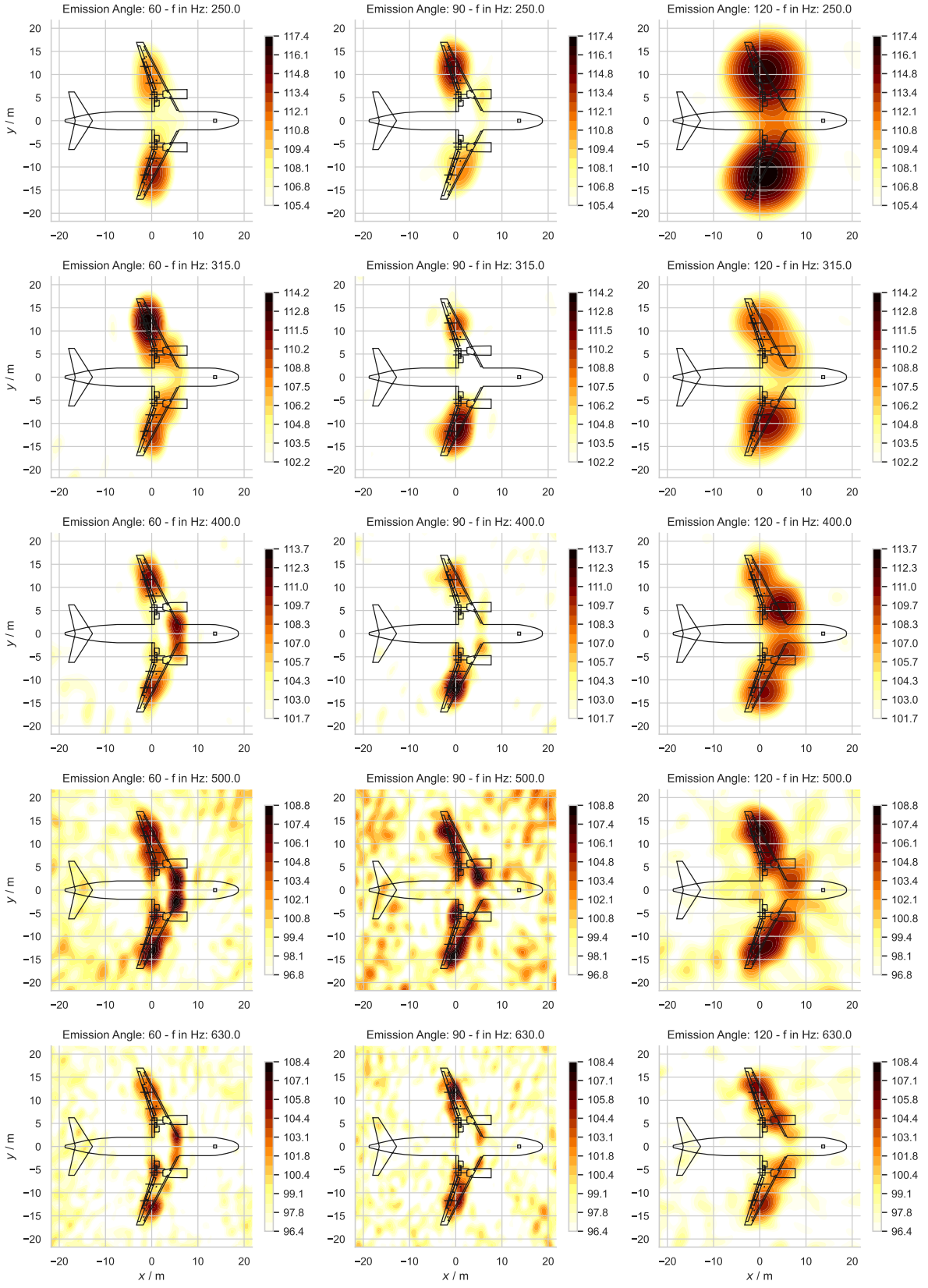

Figure 7: Beamforming results for third-octave bands 250 Hz *to* 630 Hz

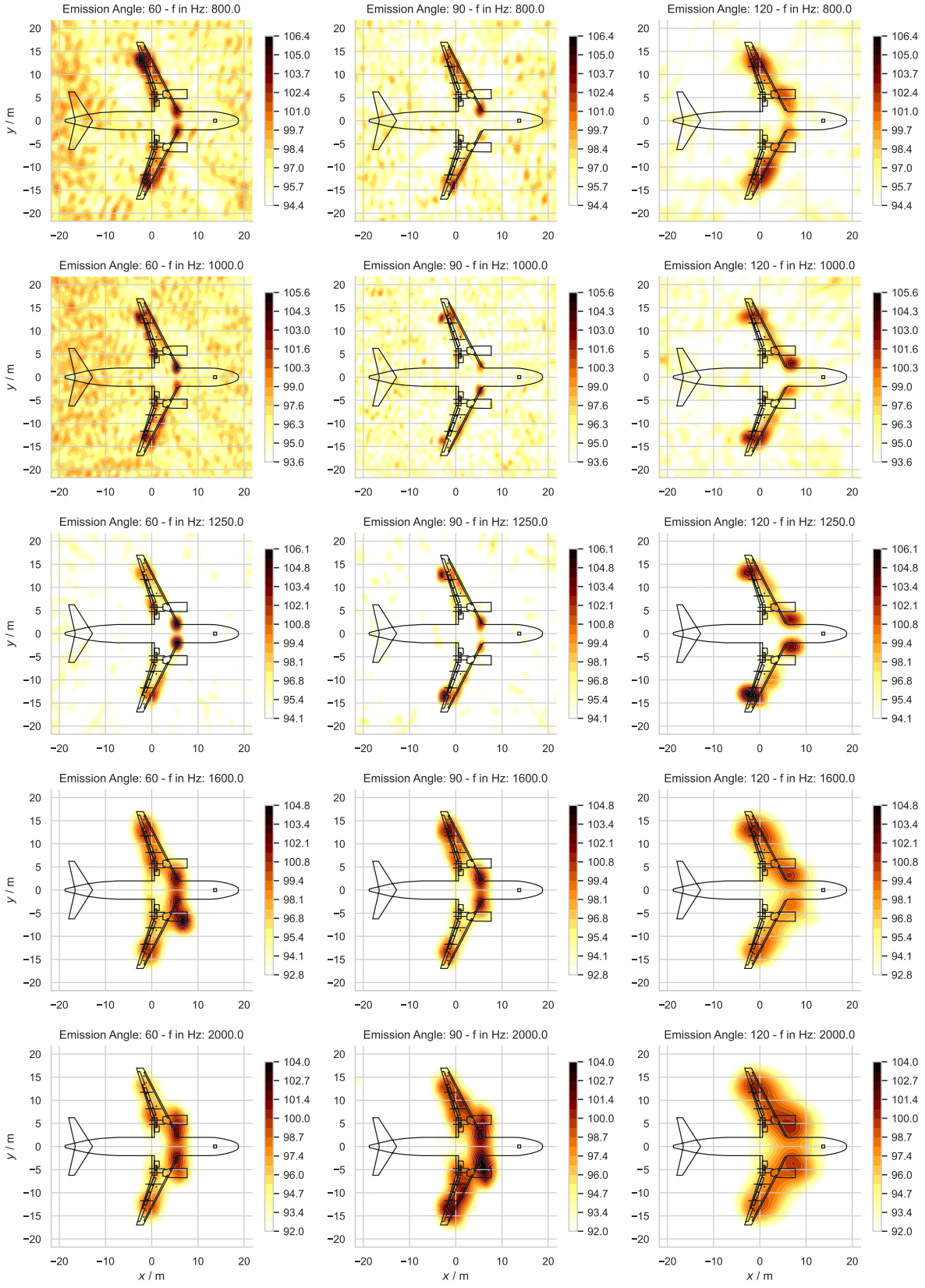

Figure 8: Beamforming results for third-octave bands 800 Hz *to* 2000 Hz

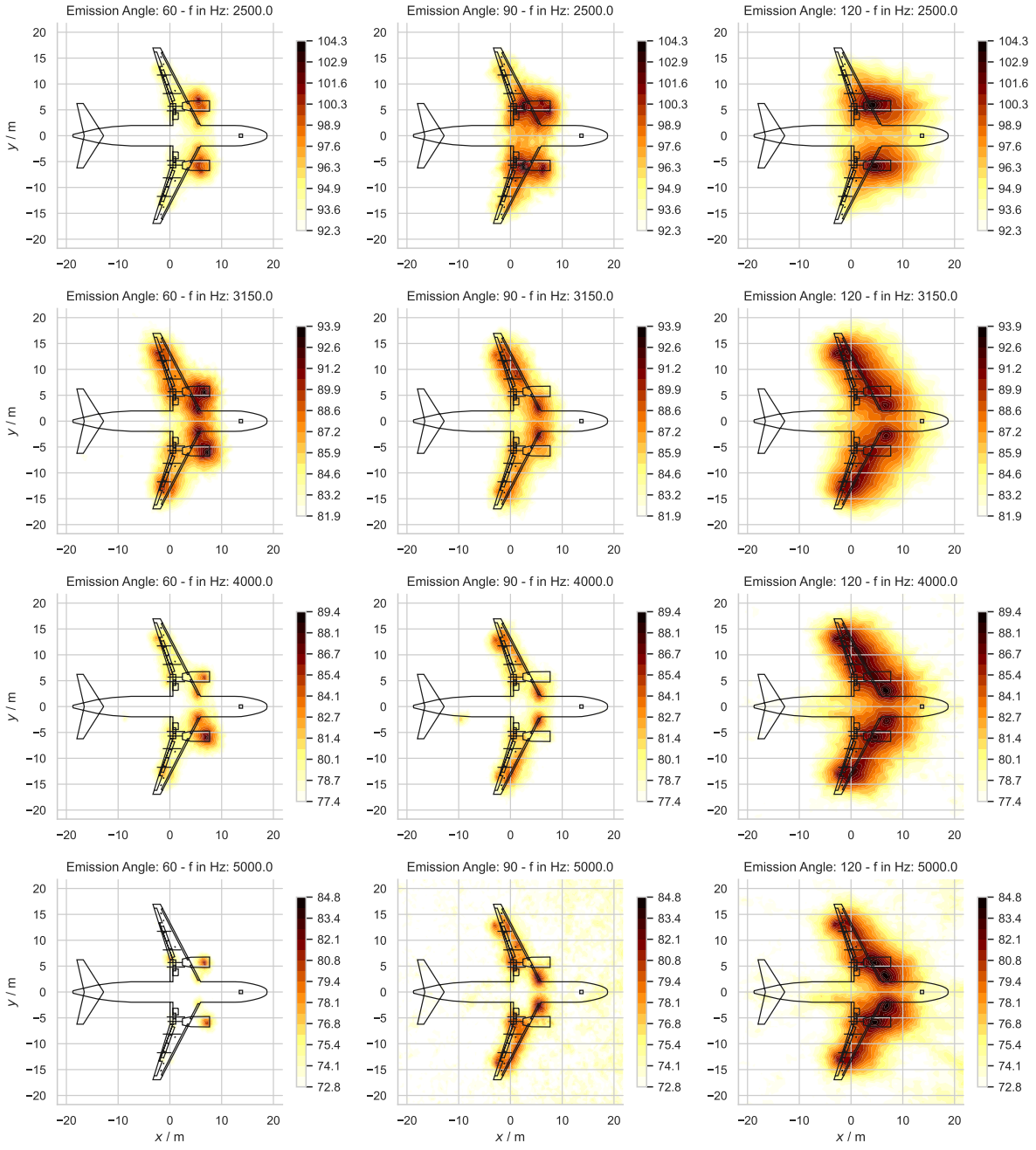

Figure 9: Beamforming results for third-octave bands 2500 Hz *to* 5000 Hz